Table 3. Continued.

Patient	Gender	DS phenotype	Last visit: Age (years)	Seizure type	Intellectual disability	Motor disability	Social outcome	Alpha rhythms	*SCN1A*: Mutation	DNA Protein
						SE at 1 year 1 month old				
27[9]	M	Typical	19	GTCS(d)	Severe	Ataxic gait	Sheltered workshop	–	Frameshift	c.5678insACTA Leu1659fsX1667
28[9]	M	Typical	32	GTCS(w)	Severe	Ataxic gait	Institutionalized	–	Frameshift	c.2841delC Asp947fsX962
29	M	Typical	19	GTCS(d), CPS	Severe	Bedridden	Institutionalized	–	Frameshift	c.5059delT F1687fsX1714
30	F	Typical	36	GTCS(m), CPS	Moderate	Unremarkable	Sheltered workshop	–	Frameshift	c.4265-8insGGGT Y1422fsX1431
31	F	Typical	28	GTCS(m)	Moderate	Ataxic gait	Sheltered workshop	–	Frameshift	c.5131delG F1710fsX1714
32	F	Typical	37	GTCS(m), CPS	Severe	Bedridden	Sheltered workshop	–	Frameshift	c.5540insAAAC L1847fsX1861
33	F	Atypical	35	GTCS(w)	Moderate	Unremarkable	Sheltered workshop	–	Frameshift	c.5108insACAT M1704fsX1709
34[11]	M	Typical	32	GTCS(y)	Severe	Unremarkable	Sheltered workshop	+		Not detected
35	M	Typical	28	GTCS(w), MS	Moderate	Ataxic gait	Sheltered workshop	–		Not detected
36[11]	F	Atypical	19	GTCS(d)	Severe	Bedridden	Sheltered workshop	+		Not detected

GTCS, generalized tonic–clonic seizures; MS, myoclonic seizures; CPS, complex partial seizures; SE, status epilepticus.
GTCS frequency: y, yearly; m, monthly; w, weekly; d, daily.
Group A: missense mutation (patients 1–18). Group B: nonsense mutation (patients 19–26), frameshift (patients 27–33).
SCN1A mutation listed for the *SCN1A* variant database.[40]

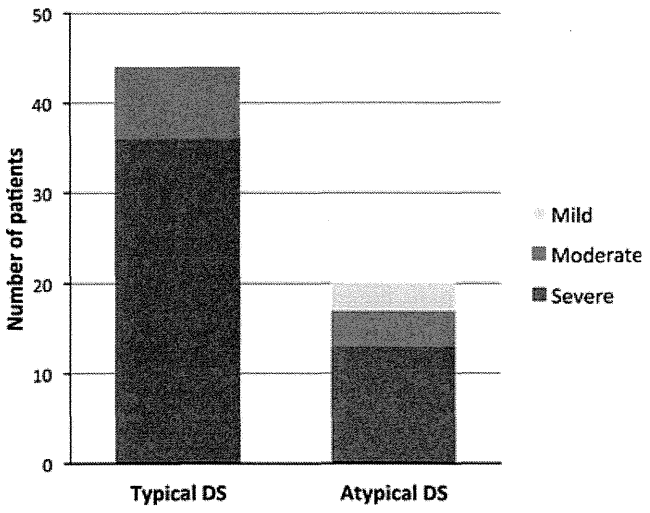

Figure 4.
Phenotypes and outcomes of intellectual disability. Patients with atypical DS tended to have milder intellectual disability compared to those with typical DS ($p = 0.0283$).
Epilepsia © ILAE

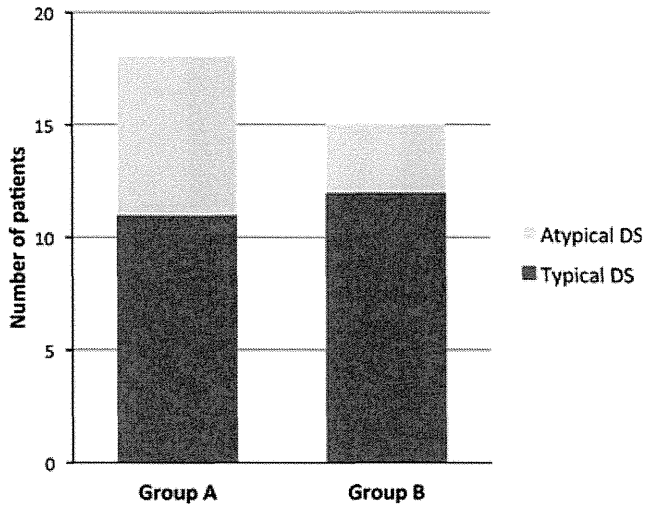

Figure 5.
Types of *SCN1A* mutations and phenotypes. Typical DS tended to be more common in group B, although this relation did not reach statistical significance ($p = 0.2828$).
Epilepsia © ILAE

was severe in 16 patients in group A and 12 patients in group B, moderate in no patients in group A and 3 patients in group B, and mild in 2 patients in group A and no patient in group B (Fig. 7).

Discussion

Compared to other epileptic encephalopathies such as West syndrome and Lennox-Gastaut syndrome, the concept of DS as an epileptic encephalopathy was established at a

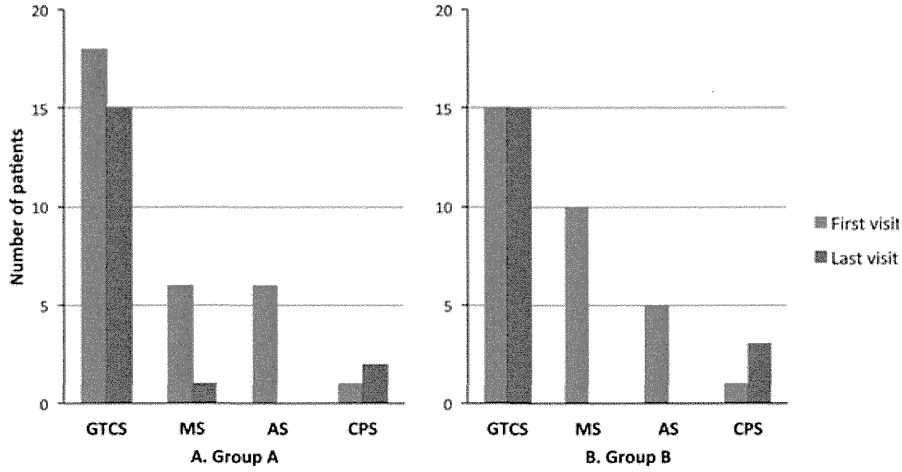

Figure 6.
Types of *SCN1A* mutations and seizure outcome. The outcomes of various seizure types were not different between the two groups. Patients with seizure freedom for 1 year or longer were found only in group A.
Epilepsia © ILAE

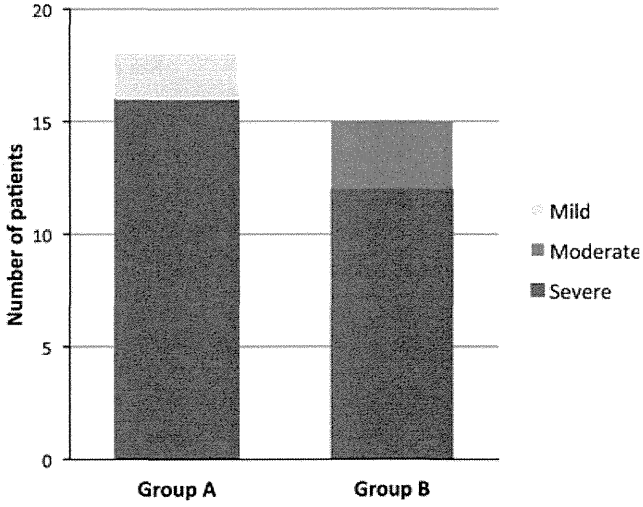

Figure 7.
Types of *SCN1A* mutations and outcomes of intellectual disability. Patients with mild intellectual disability were found only in group A.
Epilepsia © ILAE

later date, which partially accounts for the paucity of reports on the long-term course of this epilepsy syndrome. Our center, the first epilepsy center in Japan, was inaugurated in 1975. Because of the concentration of refractory epilepsy cases referred from all over Japan, we have taken an interest in a group of fever-induced intractable grand mal epilepsies (nowadays referred to as DS) from the early days. Therefore, we were in a favorable position to study the long-term course of these epilepsies in a retrospective manner. Another feature of the present study is that we were able to observe the long-term course of a cohort longitudinally at a single epilepsy center.

The long-term course of DS was studied by investigating the courses of three outcome measures: death, refractory seizures, and remission. This study is characterized by a long follow-up period of 11 years to 34 years and 5 months (median 24 years). In terms of the long-term outcome of epileptic seizures, myoclonic seizures and atypical absence seizures decreased with time, and photosensitive seizures were also reduced markedly. On the other hand, only GTCS persisted in all patients. However, the frequency of GTCS also decreased over time, and SE no longer occurred during follow-up. This trend is consistent with our previous report[17] and those of other investigators.[13,20,21] Although few in number, some patients did achieve remission of seizures. Remission was seen after 15 years of age, with the latest at 28 years. These findings indicate that epileptogenicity attenuates with age.

In the present study, the frequency of patients manifesting CPS was equally low at presentation and at the last visit. Akiyama et al.[15] reported an increase in partial seizures over time. In our study, however, we observed no increase in partial seizures. Genton et al.[16] also reported that only one of 24 patients continued to have partial seizures at the last visit. Although Genton et al.[16] reported persistence of US, we found that US disappeared in all the cases. The present finding that GTCS continued for a long period is consistent with previous reports.

Photosensitive seizures disappeared in all patients during follow-up. Although photosensitivity seen in idiopathic epilepsy is common during adolescence,[22] photosensitivity in DS is marked during infancy and is strongly manifested. The photoparoxysmal response (PPR) in patients with idiopathic general epilepsy is wave-length dependent.[23] In contrast, DS patients exhibit quantity-of-light dependent PPR.[24] The age dependence of photosensitivity in DS

patients may reflect the difference in mechanism of PPR expression.

Regarding the evolution of EEG findings, focal discharges became dominant during follow-up. Moreover, localization of spike focus in the frontal lobe became more common. However, no increase in patients with partial seizures and no evolution to frontal lobe epilepsy were observed. There was no correlation between the location of EEG focus and clinical seizures. Bureau and Dalla Bernardina[25] proposed that the interictal focal spikes lack epileptogenicity and represent fragmentary expression of diffuse discharges.

In the long-term course, there was an increase in number of patients showing reduced diffuse high potential slow waves and increase in occipital alpha rhythms. In all five patients who achieved seizure remission, occipital alpha rhythms appeared and epileptic discharges disappeared.

Because paroxysmal EEG abnormalities in DS patients can fluctuate according to the different conditions, a precise evaluation of the true incidence and frequency of the paroxysmal EEG abnormalities in DS patients is difficult.[25] In this series, five patients had no epileptic discharges both at the first and the last visit. Probably the lack of EEG recordings in young age can explain why those patients showed no or rare epileptic discharges during observation. Wide range of ages at presentation is one of the limitations of this study.

Intellectual outcome was very poor. Most patients had moderate to severe intellectual disability. The intellectual disability of the five patients with seizure remission was severe in two, moderate in one, and mild in two. Higher GTCS frequency correlated with more severe intellectual disability (Table 2).

Despite decrease of seizure severity with age, the neuropsychological outcome was poor. Akiyama et al.[15] reported a correlation between the presence of occipital alpha rhythms and mild intellectual disability. We also observed a trend of milder intellectual disability in patients with occipital alpha rhythms compared with those without.

In DS, SE has been reported to cause severe neuropsychological impairments and acute encephalopathy.[26] In our series also, permanent hemiplegia and developmental regression developed after febrile SE in four cases. Attention has to be given to severe neurologic sequelae that occur occasionally after SE in DS.

Two patients died. Mutational analysis was not performed for them. According to Sakauchi et al.,[27] sudden death peaked at 1–3 and 18 years of age, acute encephalopathy-related death peaked at 6 years, and death from drowning occurred at 7 years and above. In the present study, the ages at death were 19 years from drowning and 24 years from febrile illness–related sudden death, similar to those reported by Sakauchi et al.[27] Both cases had had GTCS, and their seizure frequency had not changed before death.

Since it became known that *SC1NA* mutation is the main cause of DS,[8–10] the relationship between genotype and phenotype has been a topic of much discussion. The phenotype-genotype correlation is complex. Zuberi et al.[28] examined >800 *SCN1A* mutations and conducted a detailed analysis on the relationship between the mutation genotype (truncating mutation or missense mutation) and phenotype. They reported that the ages of seizure onset (months after birth) for prolonged seizures, myoclonic seizures, and atypical absence seizures were earlier in patients with truncating mutation than in patients with missense mutation, suggesting that truncating mutation has greater contribution to severe phenotype than missense mutation. When the cohort was further followed and the factors associated with 5-year outcome were studied, the factors associated with poor outcome were frequent SE, EEG abnormality before 1 year of age, and motor disorder, whereas mutation class (truncating vs. missense) had no relation with outcome.[2]

There are few studies that verify the relationship between genotype and long-term course, especially the outcome in adult patients. Jansen et al.[13] reported that any particular *SCN1A* mutation type did not affect seizure outcome, but the number of cases was small. Akiyama et al.[15] investigated the relationship between long-term outcome and genotype in 25 adult patients with DS who harbored *SCN1A* mutations, and found that the mutation class had no effect on the long-term seizure and intellectual outcomes. Catarino et al.[29] reported the relationship between genotype and phenotype in adults with DS, including autopsy cases. Although all four patients with sudden death occurring during infancy had truncating mutations, two patients that died during adulthood had no mutation (one case) or missense mutation (one case) but no truncating mutation. Because missense mutation was found in milder phenotype capable of survival until adulthood, whereas truncating mutation was present in severe phenotype causing death during childhood, the potential effect of genotype class on phenotype may be speculated.

Epilepsies associated with *SCN1A* abnormalities distribute in a continuous spectrum of severity, with DS being the most severe and generalized epilepsy with febrile seizure plus (GEFS+) the least severe. DS consists of a typical type and an atypical clinical subtype. Whether seizure outcome differs between the two types of DS is not certain; we encountered no remitted cases in both types in our previous study.[17] In the present study, however, long-term follow-up of patients until adulthood revealed a difference in seizure outcome between the two phenotypes. Seizure remission is extremely rare in patients with typical DS, even after reaching adulthood.

Recently a study of cognitive development in DS was reported.[30] In this series, early appearance of myoclonus and absences was associated with the worst cognitive outcome. The authors suggest that the epilepsy phenotype has a prognostic value. In our series we found significant difference in intellectual outcome between typical DS and atypical DS ($p = 0.0283$). Patients with atypical DS tended

to have milder intellectual disability. Our results show that epilepsy phenotype influences not only seizure outcome but also intellectual outcome.

The long-term seizure and intellectual outcomes are affected by various factors interacting in a complex manner, and identification of single attributing factors is difficult. Our study is a retrospective and descriptive one. Much more research and long-term prospective studies of large numbers of patients are needed to examine the roles of various factors. The fact that the extent of damage from convulsion plays an important role in outcome has been elucidated in previous studies as well as the present results. Further research about the possible role played by different kinds of epileptic seizures on development is needed to clarify the contribution of epilepsy-related factors to the cognitive phenotype.[5]

The present study reconfirms that the long-term intellectual and seizure outcomes of DS are extremely poor except a few cases. Although DS is refractory to all the conventional AEDs, recent studies have reported the effectiveness of new drugs such as stiripentol[31,32] and topiramate. However, the patients in this series were not treated with the new drugs. It is important to avoid drugs with aggravating effects such as carbamazepine and lamotorigine.[4] Identification of the DS in the early stage would be of the utmost important to start appropriate treatment and avoid aggressive heavy medication. Simple screening test could help to predict DS.[34]

We must acknowledge that our series consisted of severe cases diagnosed a few decades ago. Current earlier recognition of DS and early initiation of suitable new drugs and further development of new effective therapies are likely to lead better outcomes.

Disclosure

None of the authors has any conflicts of interest to disclose. We confirm that we have read the Journal's position on issues involved in ethical publication and affirm that this report is consistent with those guidelines.

References

1. Hurst DL. Epidemiology of severe myoclonic epilepsy of infancy. *Epilepsia* 1990;31:397–400.
2. Brunklaus A, Ellis R, Reavey E, et al. Prognostic, clinical and demographic features in SCN1A mutation-positive Dravet syndrome. *Brain* 2012;135:2329–2336.
3. Engel J Jr. ILAE Commission Report. A proposed diagnostic scheme for people with epileptic seizures and with epilepsy: report of the ILAE task force on classification and terminology. *Epilepsia* 2001;42:796–803.
4. Dravet C, Bureau M, Oguni H, et al. Dravet syndrome (severe myoclonic epilepsy in infancy). In Bureau M, Genton P, Dravet C, Delgado-Escueta AV, Tassinari CA, Thomas P, Wolf P (Eds) *Epileptic syndromes infancy, childhood and adolescence*. 5th Ed. Montrouge: John Libbey Eurotext, 2012:125–156.
5. Guzzetta F. Cognitive and behavioral characteristics of children with Dravet syndrome: an overview. *Epilepsia* 2011;52(Suppl. 2):35–38.
6. Higashi T, Morikawa T, Seino M. A group of childhood epilepsy accompanied by refractory grand mal. *Folia Psychiatr Jpn* 1982;36:319–320.
7. Watanabe M, Fujiwara T, Terauchi N, et al. Intractable grand mal epilepsy developed in the first year of life. In Manelis J, Bentol E, Loever JN, Dreifuss FE (Eds) *Advances in epileptology: the 17th Epilepsy International Symposium*. New York, NY: Raven Press, 1989:327–329.
8. Claes L, Del-Favero J, Ceulemans B, et al. De novo mutations in the sodium-channel gene *SCN1A* cause severe myoclonic epilepsy of infancy. *Am J Hum Genet* 2001;68:1327–1332.
9. Sugawara T, Mazaki-Miyazaki E, Fukushima K, et al. Frequent mutations of SCN1A in severe myoclonic epilepsy in infancy. *Neurology* 2002;58:1122–1124.
10. Ohmori I, Ouchida M, Ohtsuka Y, et al. Siginificant correlation of the SCN1A mutations and severe myoclonic epilepsy in infancy. *Biochem Biophys Res Commun* 2002;295:17–23.
11. Fujiwara T, Sugawara T, Mazaki-Miyazaki E, et al. Mutations of sodium channel α subunit type 1 (SCN1A) in intractable childhood epilepsies with frequent generalized tonic–clonic seizures. *Brain* 2003;126:531–546.
12. Fujiwara T. Clinical spectrum of mutations in SCN1A gene: severe myoclonic epilepsy in infancy and related epilepsies. *Epilepsy Res* 2006;70(Suppl. 1):S223–S230.
13. Jansen FE, Sadleir LG, Harkin LA, et al. Severe myoclonic epilepsy of infancy (Dravet syndrome): recognition and diagnosis in adults. *Neurology* 2006;67:2224–2226.
14. Dravet C, Daquin G, Battaglia D. Severe myoclonic of infancy (Dravet syndrome). In Nikanorova M, Genton P, Sabers A (Eds) *Long-term evolution of epileptic encephalopathies*. Paris: John Libbey Eurotext, 2009:29–38.
15. Akiyama M, Kobayashi K, Yoshinaga H, et al. A long-term follow-up study of Dravet syndrome up to adulthood. *Epilepsia* 2010;51:1043–1052.
16. Genton P, Velizarova R, Dravet C. Dravet syndrome: the long-term outcome. *Epilepsia* 2011;52(Suppl. 2):44–49.
17. Fujiwara T, Watanabe M, Takahashi Y, et al. Long-term course of childhood epilepsy with intractable grand mal seizures. *Jpn J Psychiatry Neurol* 1992;46:297–302.
18. Dravet C, Bureau M, Oguni H, et al. Severe myoclonic epilepsy in infancy (Dravet syndrome). In Roger J, Bureau M, Dravet C, Genton P, Tassinari CA, Wolf P (Eds) *Epileptic syndromes in infancy, childhood and adolescence*. 4th Ed. Montrouge: John Libbey Eurotext, 2005:89–113.
19. Commission on Classification and Terminology of the International League Against Epilepsy. Proposal for revised classification of epilepsies and epileptic syndromes. *Epilepsia* 1989;30:389–399.
20. Oguni H, Hayashi K, Awaya Y, et al. Severe myoclonic epilepsy in infants- a review based on the Tokyo Women's Medical University series of 84 cases. *Brain Dev* 2001;23:736–748.
21. Dravet C, Guerrini R. Long-term outcome. In Dravet C, Guerrini R (Eds) *Dravet syndrome*. Paris: John Libbey Eurotext, 2011:83–91.
22. Shiraishi H, Fujiwara T, Inoue Y, et al. Photosensitivity in relation to epileptic syndromes: a survey from an epilepsy center in Japan. *Epilepsia* 2001;42:393–397.
23. Takahashi Y, Fujiwara T, Yagi K, et al. Wavelength specificity of photoparoxysmal responses in idiopathic generalized epilepsy. *Epilepsia* 1995;36:1084–1088.
24. Takahashi Y, Fujiwara T, Yagi K, et al. Photosensitive epilepsies and pathophysiologic mechanisms of the photoparoxysmal response. *Neurology* 1999;53:926–932.
25. Bureau M, Dalla Bernardina B. Electroencephalographic characteristics of Dravet syndrome. *Epilepsia* 2011;52(Suppl. 2):13–23.
26. Okumura A, Uematsu M, Imataka G, et al. Acute encephalopathy in children with Dravet syndrome. *Epilepsia* 2012;53:79–86.
27. Sakauchi M, Oguni H, Kato I, et al. Retrospective multiinstitutional study of prevalence of early death in Dravet syndrome. *Epilepsia* 2011;52:1144–1149.
28. Zuberi SM, Brunklaus A, Birch R, et al. Genotype-phenotype associations in *SCN1A*-related epilepsies. *Neurology* 2011;76:594–600.

29. Catarino CB, Liu JY, Liagkouras I, et al. Dravet syndrome as epileptic encephalopathy: evidence from long-term course and neuropathology. *Brain* 2011;134:2982–3010.
30. Ragona F, Granata T, Dalla Bernardina B, et al. Cognitive development in Dravet syndrome: a retrospective, multicenter study of 26 patients. *Epilepsia* 2011;52:386–392.
31. Chiron C, Marchand MC, Tran A, et al. Stiripentol in severe myoclonic epilepsy in infancy: a randomised placebo-controlled syndrome-dedicated trial. *Lancet* 2000;356:1638–1642.
32. Inoue Y, Ohtsuka Y, Oguni H, et al. Stiripentol open study in Japanese patients with Dravet syndrome. *Epilepsia* 2009;50:2362–2368.
33. Takahashi H, Takahashi Y, Mine J, et al. Effectiveness of topiramate in eleven patients with Dravet syndrome. *No To Hattatsu* 2010;42:273–276 (in Japanese).
34. Hattori J, Ouchida M, Ono J, et al. A screening test for the prediction of Dravet syndrome before one year of age. *Epilepsia* 2008;49:626–633.
35. Depienne C, Trouillard O, Saint-Martin C, et al. Spectrum of *SCN1A* gene mutations associated with Dravet syndrome: analysis of 333 patients. *J Med Genet* 2009;46:183–191.
36. Osaka H, Ogiwara I, Mazaki E, et al. Patients with a sodium channel alpha 1 gene mutation show wide phenotypic variation. *Epilepsy Res* 2007;75:46–51.
37. Mancardi MM, Striano P, Gennaro E, et al. Familial occurrence of febrile seizures and epilepsy in severe myoclonic epilepsy of infancy (SMEI) patients with *SCN1A* mutations. *Epilepsia* 2006;47:1629–1635.
38. Fujiwara T, Nakamura H, Watanabe M, et al. Clinicoelectrographic concordance between monozygotic twins with severe myoclonic epilepsy in infancy. *Epilepsia* 1990;31:281–286.
39. Sun H, Zhang Y, Liang J, et al. Seven novel *SCN1A* mutations in Chinese patients with severe myoclonic epilepsy of infancy. *Epilepsia* 2008;49:1104–1107.
40. Claes LR, Deprez L, Suls A, et al. The *SCN1A* variant database: a novel research and diagnostic tool. *Hum Mutat* 2009;30:E904–E920.

A Storm of Fast (40–150Hz) Oscillations during Hypsarrhythmia in West Syndrome

Katsuhiro Kobayashi, MD, Tomoyuki Akiyama, MD, Makio Oka, MD, Fumika Endoh, MD, and Harumi Yoshinaga, MD

Objective: Fast oscillations (FOs) were first explored from scalp electroencephalographic (EEG) data from hypsarrhythmia in West syndrome (infantile spasms) to investigate the meaning of FOs in this epileptic encephalopathy.
Methods: In 17 infants with West syndrome, we conservatively detected fast frequency peaks that stood out from the time-frequency spectral background with square root power > 1μV (spectral criterion) and corresponded to clear FOs with at least 4 oscillations in the filtered EEG traces (waveform criterion) in sleep EEGs.
Results: We found a total of 1,519 interictal FOs that fulfilled both the spectral and waveform criteria. The FOs with a median frequency of 56.6Hz (range = 41.0–140.6Hz) were dense, with a median rate of 66 (range = 24–171) per minute before adrenocorticotropic hormone (ACTH) treatment, which was significantly higher than that in control infants without seizures (median = 1, $p < 0.001$). The FOs were reduced by treatment. The mean gamma and ripple oscillation rates that were detected using the waveform criterion alone were 40.62/min and 15.75/min, respectively, per channel; these results were 112.8 and 98.4 times higher, respectively, than the previously reported corresponding rates in adult epilepsy patients.
Interpretation: The observed FOs corresponded to epileptogenicity because of their close relation to the severity of hypsarrhythmia during the course of ACTH treatment. The very high epileptic FO rates in hypsarrhythmia are thought to affect the process of neurodevelopment by interfering with physiological functions in West syndrome, taking into account that high frequencies are also important in physiological higher brain functions.

ANN NEUROL 2015;77:58–67

West syndrome is a representative type of infantile epileptic encephalopathy characterized by a combination of epileptic spasms (infantile spasms), arrest of psychomotor development, and the unique interictal electroencephalographic (EEG) abnormality of hypsarrhythmia. The principal features of hypsarrhythmia are very high amplitude and irregular slow waves with superimposed multifocal epileptic spikes. West syndrome is a grave clinical problem for infants because of its poor developmental prognosis, but the pathophysiological mechanisms involved in West syndrome that cause neurodevelopmental impairments are yet to be fully understood. We found fast oscillations (FOs) in the ictal scalp EEG data of epileptic spasms.[1,2] It was subsequently demonstrated that cortical high-frequency oscillations (HFOs) are observed in association with spasms corresponding to the scalp FOs.[3,4]

High-frequency electrical activities are suggested to play a crucial role in both physiological and pathological brain functions. Regarding the physiological functions, cerebral activity in gamma and higher frequency bands is thought to play an important role in higher brain functions.[5–8] Conversely, pathological HFOs are related to epileptogenesis.[9–17] HFOs include ripples (80–200 or 250Hz) and fast ripples (200 or 250–500Hz), and were shown to have an even closer relationship with epileptogenicity and ictogenicity than epileptic spikes have.[18] FOs including gamma (40–80Hz) and ripple oscillations were shown to be recordable over the scalp,[19–24] which is expected to expand the clinical utility of high frequencies in EEG data.

View this article online at wileyonlinelibrary.com. DOI: 10.1002/ana.24299

Received Jul 2, 2014, and in revised form Oct 18, 2014. Accepted for publication Oct 26, 2014.

Address correspondence to Dr Kobayashi, Department of Child Neurology, Okayama University Hospital, Shikatacho 2-chome 5-1, Kita-ku, Okayama 700–8558, Japan. E-mail: k_koba@md.okayama-u.ac.jp

From the Department of Child Neurology, Okayama University Graduate School of Medicine, Dentistry, and Pharmaceutical Sciences and Okayama University Hospital, Okayama, Japan.

Additional Supporting Information may be found in the online version of this article.

In our initial study on FOs in the ictal EEG data of epileptic spasms, we could not detect FOs from the interictal hypsarrhythmia using rather primitive analytic techniques with a low-cut frequency filter at 5.3Hz.[1] Analytic methods have developed during the past decade, and in the current study, we explored FOs from hypsarrhythmia, a matter that, to our knowledge, has not previously been studied. We herein report that there were large numbers of FOs in hypsarrhythmia with rates that were beyond those previously observed in adult patients with epilepsy.[21]

Subjects and Methods

Subjects

Subjects in this study were 17 infants with West syndrome (7 boys, 10 girls), who were treated at the Okayama University Hospital from 2008 to 2012. Age at the initial EEG recording ranged from 3 to 9 months (mean = 5.8 months). All the patients showed hypsarrhythmia in the interictal EEG. The occurrence of epileptic spasms in series was confirmed using video-EEG monitoring in 16 patients, and subclinical ictal EEG patterns were recorded in the remaining 1. The patients had various etiologies. We excluded patients who had focal features in hypsarrhythmia and/or the ictal EEGs, and previously reported patients.[1,25] Demographic data from these infants are presented in the Supplementary Table. This study was approved by the Okayama University Ethics Committee.

We treated the patients with a protocol in which low-dose tetracosactide Zn (synthetic adrenocorticotropic hormone [ACTH]; Cortrosyn Z) at a dose of 0.005mg/kg/day was initially administered for 2 weeks, and, if seizures and/or intense EEG abnormalities continued, higher dose ACTH (0.025mg/kg/day) was administered for an additional 2 weeks. All patients in this study eventually received ACTH for a total of 4 weeks. Clinical seizures were at least temporarily suppressed by this treatment in 13 patients (76.5%). Vigabatrin, although officially unavailable in Japan, was administered to 2 patients as part of a clinical trial after the ACTH treatment.

EEG Recording

EEG was recorded for the analysis at 3 points: before the start of ACTH, when hypsarrhythmia was observed; after 2 weeks of treatment, when hypsarrhythmia was gradually subsiding; and after 4 weeks of treatment, when hypsarrhythmia was largely suppressed in most patients. EEG was recorded using the international 10–20 electrode system (Neurofax; Nihon-Kohden, Tokyo, Japan), with a sampling rate of 500Hz. A low-cut frequency filter at 0.016Hz was used before digital sampling. We initially reviewed sleep EEG using a bipolar montage including the derivations of Fp1-F7, Fp2-F8, F3-C3, F4-C4, T3-T5, T4-T6, P3-O1, and P4-O2 to select clean data without apparent artifacts nor muscle activity. We used these derivations in conformity to our previous studies[1,2] with an intention to cover the electrodes in each hemisphere without duplication of electrodes. FOs were detected irrespective of polarity, and therefore FOs occurring at a given electrode should be observed no matter which bipolar electrode combination might be involved.

EEG Analysis

In each EEG record, we investigated the interictal non–rapid eye movement sleep data with a duration of 60 seconds including minimum artifacts in the bipolar derivations mentioned above. We used low-cut frequency filters at 40 and 80Hz in addition to the ordinary filter at 0.5Hz. A finite-impulse response filter was used to minimize ringing. Time-frequency analysis was performed based on the Gabor transform, which is the Fourier transform with a sliding 50-millisecond full-width at half maximum Gaussian window.[1,26] The frequency range was 20 to 150Hz. The spectral data with the corresponding filtered EEG traces were shown in a sliding window with a width of 3 seconds. The Fourier transform was performed on 256 data points (512 milliseconds; spectral resolution = 1.9Hz) at each 4-millisecond time point. We used square root power in microvolt units, which corresponded to EEG amplitude.

We identified an FO spectral peak with a power (1μV at minimum) greater than that at any other point in a given search area of the time-frequency spectrum with a temporal extent of 100 milliseconds (50 milliseconds before and 50 milliseconds after the peak) and a frequency extent of 20Hz (10Hz higher and 10Hz lower than the peak); this was a spectral criterion. The identified spectral peaks were therefore separated by at least 50 milliseconds and/or 10Hz. These criteria were systematically searched for over the entire time-frequency spectrum >40Hz to determine candidate peaks. Each candidate peak was then visually investigated to select 1 that corresponded to a clear FO with at least 4 consecutive oscillations and an amplitude markedly greater than the surrounding signals in the combined filtered and unfiltered traces (waveform criterion). The waveform pattern of FO was systematically identified by searching a run of ≥4 oscillations with peak signals of identical polarity that had amplitudes higher than a predetermined threshold and intervals within a predetermined range in the filtered EEG traces. The amplitude thresholds for gamma and ripple oscillations were arbitrarily assigned at 5 and 15 times, respectively, the root mean square (RMS) amplitude of 1-second background data, so as to represent our visual identification of markedly strong signals. The interval range of oscillations was set at 12.5 to 25 milliseconds (corresponding to wavelengths of 80 and 40Hz signal, respectively) for gamma oscillations and 6.7 to 12.5 milliseconds (corresponding to wavelengths of 150 and 80Hz signal, respectively) for ripple oscillations. The minimum separation distance between FOs was 50 milliseconds. Automatically detected FOs were visually confirmed to have clear oscillations. The background was defined as a segment of EEG data from the same record as the analyzed data but containing minimal abnormalities and artifacts. The background in hypsarrhythmia was assumed to represent a segment of EEG with fewer abnormalities that occurred between groupings of discharges during sleep.[27] FOs were identified through consensus of 2 experienced neurophysiologists. We performed this procedure to define unambiguous peaks in both power and

frequency, and our process was more conservative than that of Andrade-Valenca et al[21] for adult patients because of the additional spectral criterion used. Each spectral peak was examined whether or not it was associated with an epileptic spike. Confounding EEG background noise including artifacts and muscle activity was excluded from the analysis. We already confirmed that alternating current (AC) at 60Hz has monotonous spectral characteristics, which are different from those of epileptic FOs.[1] We also counted FOs using the waveform criterion alone according to the pre-ACTH treatment EEG data that were compared with previously reported data from adult patients.

Before the start of ACTH treatment, we recorded the ictal EEGs of epileptic spasms from 11 patients and analyzed all those that were clean enough. Ten spasms in each patient were analyzed in a similar manner (3 seconds of data for each spasm) in the derivations of F3-C3, F4-C4, P3-O1, and P4-O2. The other derivations were excluded because electrodes Fp1 and Fp2 are close to the frontalis muscle and F7, F8, T3, T4, T5, and T6 to the temporalis muscle. We have learned through experience in previous studies[1,2] that these derivations tend to be contaminated by muscle activity.

Frequencies of spectral peaks were categorized as gamma 1 (40–60Hz), gamma 2 (60–80Hz), and ripple bands (80–150Hz). Computation was performed using a program that was written in-house for Matlab (v7.5.0; MathWorks, Natick, MA).

Control Data

Control sleep EEG data were recorded from 17 infants (12 boys, 5 girls) with no seizure disorders nor EEG abnormalities in the same age range (ie, 3–9 months, mean = 5.8 months) during the same period (2008–2012). These infants were subjected to EEG for differentiation of abnormal movements or apnea from seizures in 12 cases and because of developmental retardation and/or suspected brain dysfunction in the other 5. Recording and analysis procedures were the same as those in the patients with West syndrome.

Statistical Analysis

We statistically compared the number of spectral peaks, peak power values, and peak frequencies in the EEG data recorded before the ACTH treatment, after 2 weeks of the treatment, and after 4 weeks of the treatment. These parameters were also compared between the interictal EEG data before the treatment and the ictal EEG data of epileptic spasms, and between the brain regions. The detected FOs were similarly compared between the interictal EEG data of the infants with West syndrome before the ACTH treatment and the control infants. We performed nonparametric tests (the Wilcoxon test for single comparisons and the Steel–Dwass test for multiple comparisons) because the obtained spectral data had thresholds (1μV in power and 40Hz in frequency) and therefore likely had non-Gaussian distributions. We used the JMP Japanese v11 (SAS Institute, Japan, Tokyo) for statistical analysis.

Results

We found a total of 1,519 FOs that fulfilled both the waveform and spectral criteria in the interictal EEG data showing hypsarrhythmia or its residues. Of these, 1,415 (93.2%) were associated with spikes (see Fig 1A for example; corresponding raw EEG trace in Fig 2) and the remaining 104 (6.8%) were not associated with spikes (Fig 1B for example; corresponding raw EEG trace in Fig 3). The ictal EEGs of epileptic spasms showed 639 intense FOs. Although FOs were investigated in the filtered traces, they were observed in some unfiltered ictal EEG traces as well (Fig 1C for example; corresponding raw and temporally expanded EEG traces in Fig 4). FOs observed in the control EEGs were actually phasic augmentation of background fast activity in the gamma 1 band. Artifacts and noise were carefully identified and excluded from the study.

Before ACTH treatment, the number of observed FOs was high, with a median value of 66 per 60 seconds per patient (31 in the gamma 1 band, 15 in the gamma 2 band, and 7 in the ripple band; range = 24–171). After 2 weeks of ACTH treatment, the median number had significantly decreased to 4 (3 in the gamma 1 band, 0 in the other bands; range = 0–126); at the same time, amelioration of hypsarrhythmia was observed ($p = 0.003$). After 4 weeks of the treatment, the median number had significantly decreased to 0 (0 in all bands; range = 0–11; $p < 0.001$). The reduction in the numbers of FOs in each frequency band over the first 2 weeks of treatment was statistically significant in the gamma 2 ($p = 0.013$) and ripple bands ($p = 0.007$), and that over the 4 weeks of treatment was statistically significant in the gamma 1 ($p < 0.001$), gamma 2 ($p < 0.001$), and ripple bands ($p = 0.003$). Of the 47 FOs that were observed after 4 weeks of treatment, 37 (78.7%) were observed in the 4 patients who persistently showed hypsarrhythmia or intense spikes. In the pre-ACTH treatment state, the number of FOs was significantly higher in the gamma 1 band than in the ripple band ($p < 0.001$). In the epileptic spasm ictal EEG data, the number of FOs was significantly higher in the gamma 2 band than in the gamma 1 band ($p = 0.011$; Fig 5). FOs in the control data were few, with a median value of 1 per 60 seconds per infant (range = 0–12). The FO distribution between the control data and the pre-ACTH data in the infants with West syndrome was significantly different ($p < 0.001$); in the control data, the FOs were all in the gamma 1 band and nonexistent in the gamma 2 and ripple bands ($p < 0.001$ in all bands).

Interictal FO square root power was not significantly different between the pre-ACTH treatment state and after 2 and 4 weeks of treatment in any frequency band in the patients with West syndrome. Interictal power values were significantly higher in the gamma 1 band (median = 1.52μV, range = 1.00–17.67μV) than in

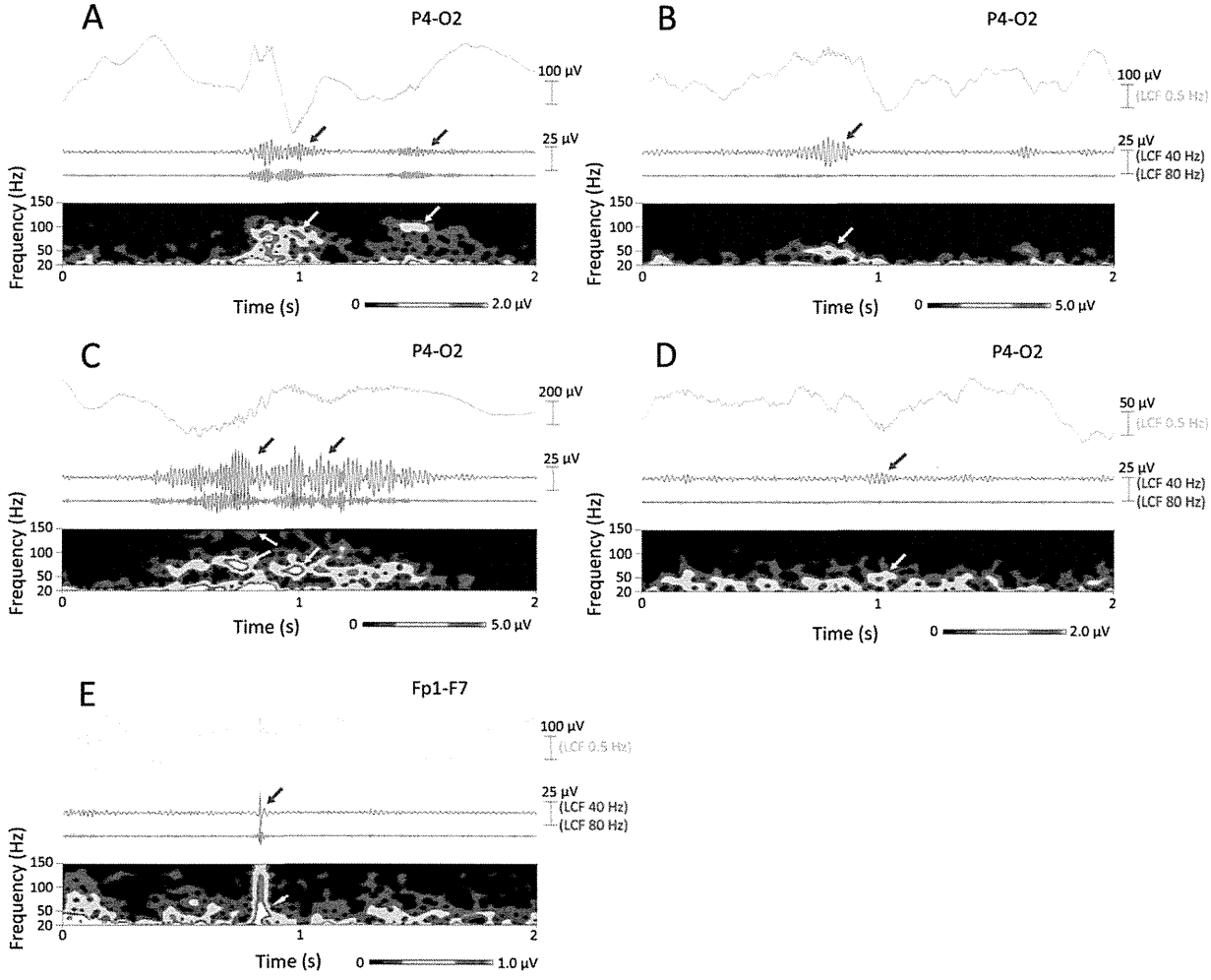

FIGURE 1: Representative fast oscillations (FOs). Electroencephalographic (EEG) traces in bipolar derivations are low-cut filtered (LCF) at 0.5Hz *(green traces)*, 40Hz *(blue traces)*, and 80Hz *(red traces)*. (A) FOs associated with spikes in hypsarrhythmia (P4-O2) recorded before the adrenocorticotropic hormone (ACTH) treatment. FOs are observed in filtered traces *(blue arrows)* and correspond to spectral blobs in the time-frequency analysis *(yellow arrows;* raw EEG trace in Fig 2). (B) FOs unassociated with spikes in hypsarrhythmia (P4-O2) that were recorded before the ACTH treatment. FOs are similarly found in filtered traces and correspond to spectral blobs *(arrows;* raw EEG trace in Fig 3). (C) FOs detected from the ictal EEG of epileptic spasms. They are clearly observed not only in the filtered traces *(blue arrows)* and the spectrum *(yellow arrows)* but also in the unfiltered EEG trace *(green trace;* raw EEG trace in Fig 4). (D) An FO observed in control EEG data recorded from an infant without seizures. (E) An artifact *(arrows)* that does not have oscillatory characteristics nor narrow band spectral blobs. It was therefore excluded from the analysis.

the ripple band (median = 1.32μV, range = 1.01–3.17μV) in the pre-ACTH treatment state ($p < 0.001$). Power values of the ictal FOs were significantly higher in the gamma 1 band (median = 3.71μV, range = 1.27–7.32μV) and the gamma 2 band (median = 3.34μV, range = 1.03–9.05μV) than in the ripple band (median = 2.43 μV, range = 1.01–9.97μV; both $p < 0.001$). They were significantly higher than those of the interictal FOs before the treatment in all frequency bands (all $p < 0.001$). Power values of FOs unassociated with spikes were lower (median = 1.31μV, range = 1.00–3.75μV) than those of FOs associated with spikes (median = 1.57μV, range = 1.00–17.67μV) in the gamma 1 band ($p < 0.001$), but they were similar in the gamma 2 and ripple bands. The median power value of FOs in the gamma 1 band in the control data was 1.26μV (range = 1.01–1.77μV), significantly lower than that in hypsarrhythmia in the pre-ACTH treatment state ($p = 0.004$). There were no accumulations of peaks at 60Hz, which exactly corresponded to AC.[1]

Frequency-dependent distributions of FOs are depicted in Figure 6. The median frequency in the infants with West syndrome was 56.6Hz (range = 41.0–140.6Hz) in the pre-ACTH treatment state, which significantly decreased to 50.8Hz (range = 41.0–97.7Hz, $p < 0.001$) after 2 weeks of treatment and to 46.9Hz (range = 41.0–84.0Hz, $p < 0.001$) after 4 weeks of treatment. FO frequencies were significantly higher in the ictal EEG data of epileptic spasms (median = 72.3Hz,

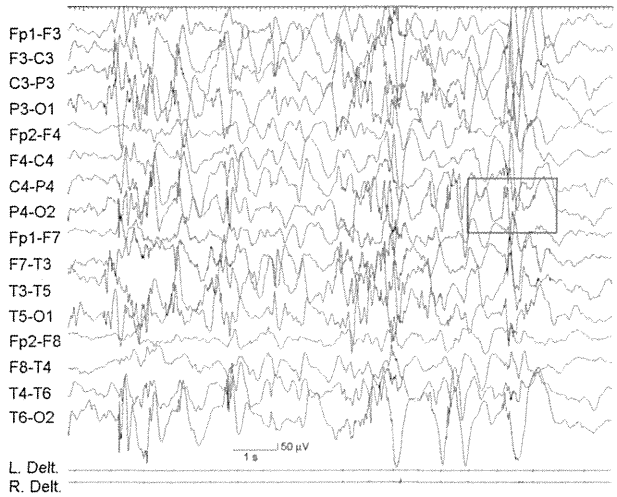

FIGURE 2: A raw electroencephalographic (EEG) trace of hypsarrhythmia including fast oscillations indicated in Figure 1A. The EEG segment in the box is magnified in Figure 1A. Delt. = deltoid muscle.

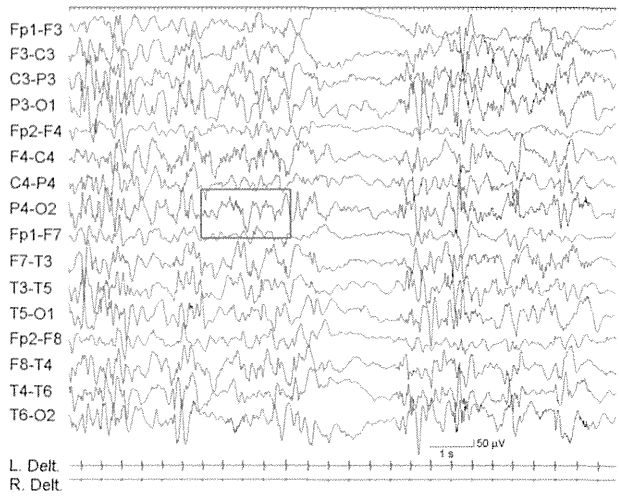

FIGURE 3: A raw electroencephalographic (EEG) trace of hypsarrhythmia including fast oscillations indicated in Figure 1B. The EEG segment in the box is magnified in Figure 1B. Delt. = deltoid muscle.

range = 41.0–144.5Hz) than in the interictal data in the corresponding derivations before ACTH treatment (median = 56.6Hz, range = 41.0–140.6Hz; $p < 0.001$). FO frequencies unassociated with spikes were lower (median = 47.9Hz, range = 41.0–101.6Hz) than those associated with spikes (median = 60.5Hz, range = 41.0–115.2Hz; $p < 0.001$). The median frequency of FOs in the control data was 43.0Hz (range = 41.0–48.8Hz), a value significantly different from that in the pre-ACTH treatment data showing hypsarrhythmia ($p < 0.001$).

For FO spatial distribution across brain regions, frequencies of the interictal FOs were slightly higher in the combined derivations of P3-O1/P4-O2 (median frequency = 58.6Hz) compared with Fp1-F7/Fp2-F8 (median = 52.7Hz, $p = 0.002$) and with F3-C3/F4-C4 (median = 53.7Hz, $p = 0.044$), and slightly higher in T3-T5/T4-T6 (median = 56.6Hz) compared with Fp1-F7/Fp2-F8 ($p = 0.022$) in the pre-ACTH treatment state. Frequencies of the ictal FOs were not significantly different between the brain regions (Fig 7). Power of FOs was not different across brain regions.

With respect to FOs that were detected using the waveform criterion alone, we found a total of 5,524 gamma oscillations (mean = 40.62 ± 33.14/min per channel) and 2,142 ripple oscillations (mean = 15.75 ± 21.46/min per channel). Compared to the previously reported data in adult patients, which indicate that the mean rates of gamma and ripple oscillations are 0.36 ± 0.83/min and 0.16 ± 0.54/min, respectively, in a total of 443 channels,[21] the rates of gamma and ripple oscillations in hypsarrhythmia in our study were 112.8 and 98.4 times the adult rates, respectively, and these differences were statistically significant (both $p < 0.001$ using an unpaired t test).

Discussion

We found a high rate of FOs in scalp EEG data showing hypsarrhythmia before the ACTH treatment even using conservative waveform and spectral criteria. The rates of gamma and ripple oscillations were significantly higher in infants with West syndrome than in the control infants without seizures, and significantly higher than in adult epilepsy patients when they were directly compared using only the waveform criterion. FOs observed in the control data had frequencies < 50Hz and appeared essentially different from the pathological FOs seen in West syndrome. Such FOs in hypsarrhythmia should represent at least some aspect of the epileptogenicity of West syndrome, as most of the observed FOs coincided with spikes, and FOs decayed in number in association with the suppression of hypsarrhythmia and epileptic spasms. It is still unclear whether FOs were actually directly calmed by treatment, given that hypsarrhythmia also disappeared and that the behaviors of FOs and hypsarrhythmia could not be investigated separately. These results may vary depending on the electrode derivations and the methodology of FO identification used for analysis. This possibility of derivation- and methodology-dependent differences in FOs will be addressed in the future. Muscle activity contamination of EEG data recorded from electrodes close to muscles, particularly in the ictal EEGs, is another problem that needs to be solved.

The pathophysiological mechanisms of neurodevelopmental impairment in West syndrome remain unknown. Infants may experience mental improvements when epileptic spasms are suppressed,[28,29] as shown both in previous studies and in Patients #11 and #13 in the current study, but it is difficult to evaluate the effects of

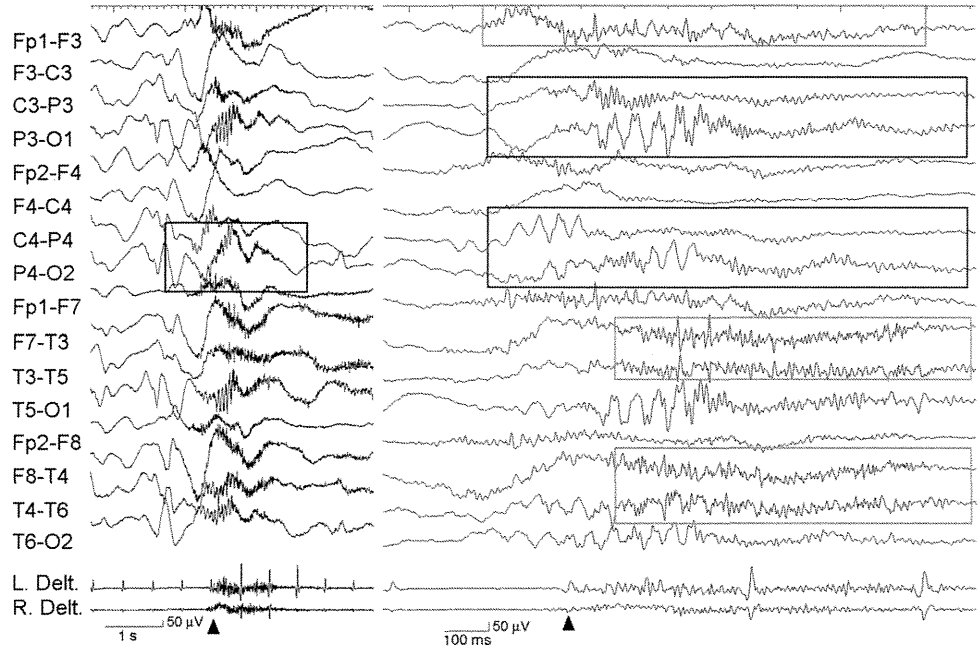

FIGURE 4: The ictal electroencephalographic (EEG) trace of an epileptic spasm including fast oscillations (FOs) indicated in Figure 1C. Left: A raw EEG trace. The EEG segment in the box is magnified in Figure 1C. Right: A temporally expanded trace of the same EEG data with a low-cut frequency filter at 5.3Hz. The 2 arrowheads indicate the identical onset time point of spasm. Part of EEG in the dark gray boxes shows FOs with rhythmic morphology. In contrast, part of EEG in the pale gray boxes includes irregular fast activity of possible muscle origin in the frontopolar and temporal regions.

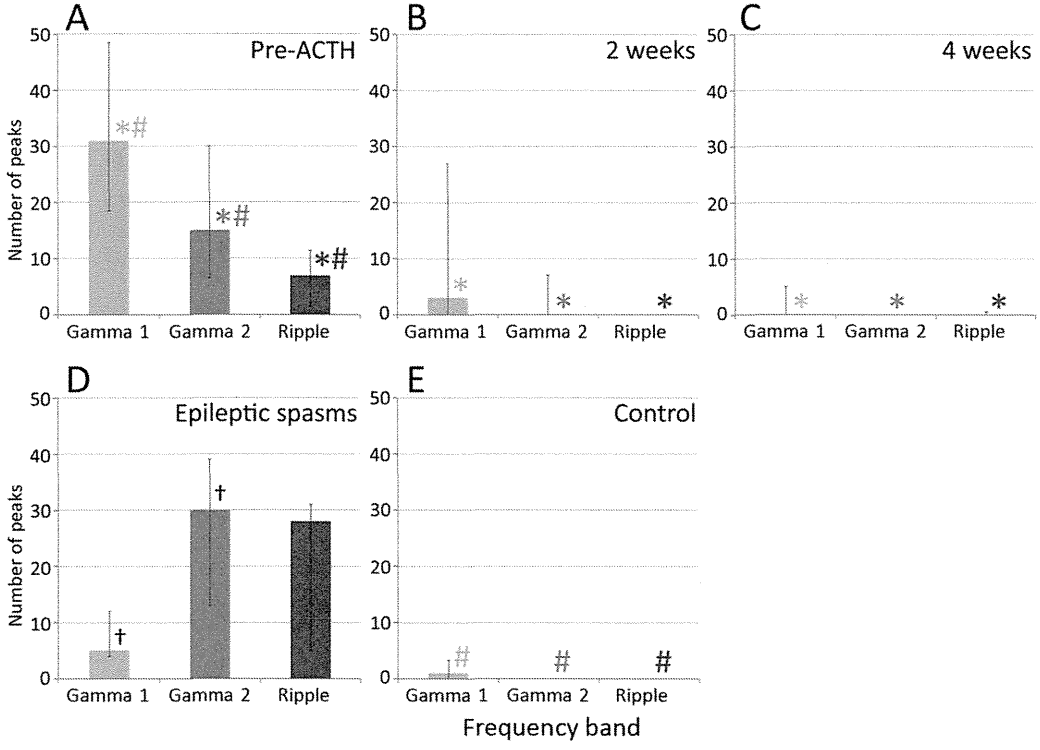

FIGURE 5: Number of fast oscillation peaks across frequency bands. The median number of peaks in individual patients with West syndrome in each frequency band is plotted according to (A) the pre–adrenocorticotropic hormone (ACTH) treatment state, (B) the state after 2 weeks of the treatment, (C) the state after 4 weeks of the treatment, and (D) the ictal electroencephalogram of epileptic spasms. (E) The median number of peaks in the control patients is also plotted. The vertical bars indicate the 25th and 75th percentiles in numbers of peaks. Asterisks in pale, medium, and dark gray indicate a corresponding pair of statistical significance between A and B and between A and C in gamma 1, gamma 2, and ripple bands, respectively. #Similar significance between A and E. †Significant difference between the gamma 1 and 2 bands in D.

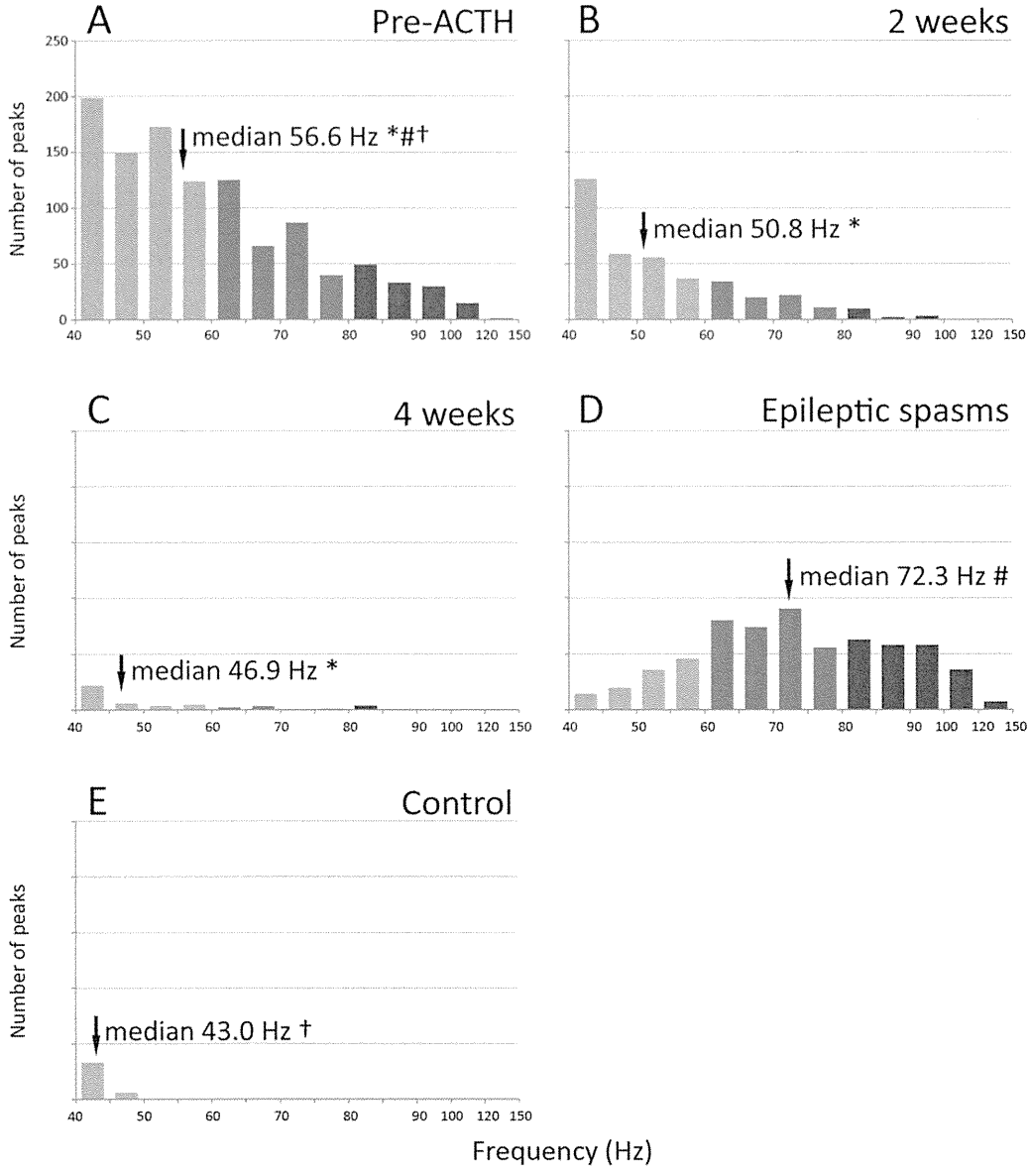

FIGURE 6: Histograms showing the distribution of fast oscillation peaks against frequency. The numbers of peaks in gamma 1, gamma 2, and ripple bands are indicated in pale, medium, and dark gray, respectively. (A) The pre–adrenocorticotropic hormone (ACTH) treatment state, (B) the state after 2 weeks of the treatment, (C) the state after 4 weeks of the treatment, and (D) the ictal electroencephalogram of epileptic spasms in patients with West syndrome. (E) The control data. *#†Pairwise statistical significance.

spasms and hypsarrhythmia separately. FOs observed over the scalp were shown to correspond to intracranial HFOs.[30,31] Animal experiments showed that pathological HFOs are associated with clusters of neuronal firing.[9] Excessive FO occurrences in hypsarrhythmia indicate overwhelming generation of pathological HFOs, which may indicate unusually active neuronal firing with bombardment effects on the neuronal system. The generation of FO storms is probably harmful to the immature brains of these patients.

It may be difficult for physiological high-frequency activity to escape being influenced by strong bombardment with pathological high-frequency activity. High-frequency activities have been demonstrated to be involved in a variety of higher brain functions, such as memory, language, and cognitive functions, particularly through intracranial EEG analysis.[5–8] Physiological high frequencies have been suggested as an index of cortical processing; they may represent an increase in global firing rates in the underlying neural system, they may function to bind together the multiple features of information through synchronous neural communication, and they may indicate large-scale causal interactions between remote cortical regions.[32,33] Physiological high

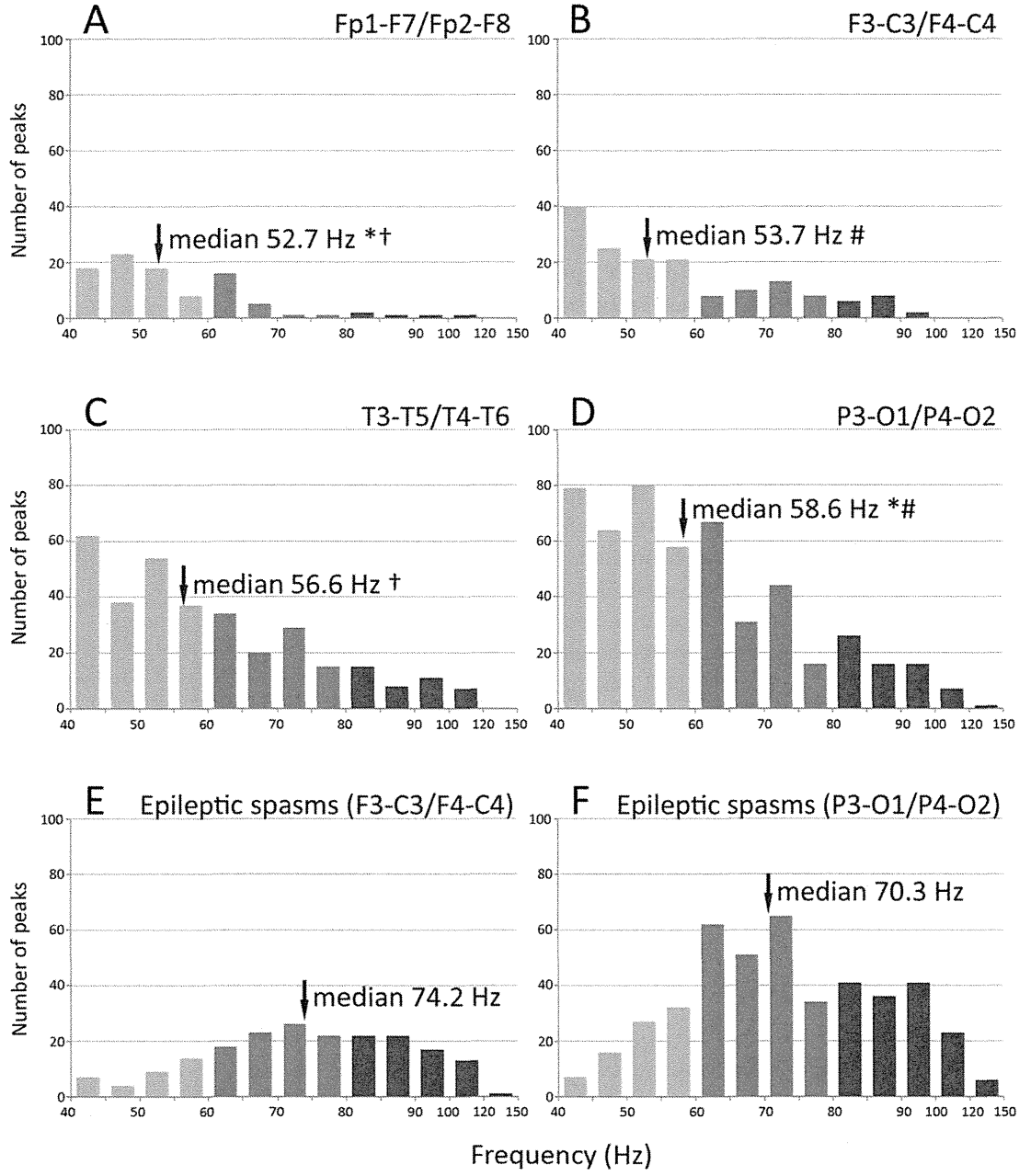

FIGURE 7: Histograms showing the distribution of fast oscillation peaks against frequency across brain regions. The numbers of peaks in gamma 1, gamma 2, and ripple bands are indicated in pale, medium, and dark gray, respectively. The interictal data before the adrenocorticotropic hormone treatment are plotted according to the combined derivations of (A) Fp-F7 and Fp2-F8, (B) F3-C3 and F4-C4, (C) T3-T5 and T4-T6, and (D) P3-O1 and P4-O2. Similar data in the ictal electroencephalograms of epileptic spasms are indicated according to the combined derivations of (E) F3-C3 and F4-C4 and (F) P3-O1 and P4-O2. *#†Pairwise statistical significance.

frequencies must play fundamental roles in higher brain function, which suggests that higher brain function might be vulnerable to pathological high-frequency attacks.

The current study excluded patients who exhibited hypsarrhythmia with focal and/or asymmetric features, because we focused on the general tendencies of FOs in hypsarrhythmia. FOs tended to be higher in frequency in the parieto-occipital derivations, corresponding to the general tendency toward posterior dominance in hypsarrhythmia.[34] It is important to identify patients who have localized lesions such as focal cortical dysplasia and who would be candidates for surgical treatment. Scalp FOs are thought to indicate the seizure onset zone.[19,21,25] Future research will include investigating the relationship of localizations between FOs in hypsarrhythmia and cortical lesions that are responsible for generating seizures.

The FOs involved in the ictal EEGs of epileptic spasms were more powerful and had higher frequencies than those in hypsarrhythmia, and were possibly the clearest type of FOs in the scalp EEGs.[1] Epileptic spasm and hypsarrhythmia generation should be linked with common observation of FOs. In hypsarrhythmia, there may be ongoing functional abnormalities represented by many FOs, which would occasionally culminate to generate spasms with greater FOs by way of a complex interaction involving both the cortex and subcortical structures. This hypothesis needs further investigation.

Acknowledgment

K.K. was supported by a research grant (24-7) for Nervous and Mental Disorders from the Ministry of Health, Labor, and Welfare, Japan; by the Japanese Health and Labor Sciences research grant "Research on catastrophic epilepsy in infancy and early childhood—epidemiology, diagnosis and treatment guide"; and by a grant-in-aid from the Ministry of Education, Culture, Sports, Science, and Technology, Japan (No. 24591513). H.Y. was supported by the Japan Epilepsy Research Foundation.

Potential Conflicts of Interest

Nothing to report.

References

1. Kobayashi K, Oka M, Akiyama T, et al. Very fast rhythmic activity on scalp EEG associated with epileptic spasms. Epilepsia 2004;45:488–496.
2. Inoue T, Kobayashi K, Oka M, et al. Spectral characteristics of EEG gamma rhythms associated with epileptic spasms. Brain Dev 2008;30:321–328.
3. Akiyama T, Otsubo H, Ochi A, et al. Focal cortical high-frequency oscillations trigger epileptic spasms: confirmation by digital video subdural EEG. Clin Neurophysiol 2005;116:2819–2825.
4. Nariai H, Nagasawa T, Juhász C, et al. Statistical mapping of ictal high-frequency oscillations in epileptic spasms. Epilepsia 2011;52:63–74.
5. Axmacher N, Elger CE, Fell J. Ripples in the medial temporal lobe are relevant for human memory consolidation. Brain 2008;131:1806–1817.
6. Brown EC, Rothermel R, Nishida M, et al. In-vivo animation of auditory-language-induced gamma-oscillations in children with intractable focal epilepsy. Neuroimage 2008;41:1120–1131.
7. Herrmann CS, Fründ I, Lenz D. Human gamma-band activity: a review on cognitive and behavioral correlates and network models. Neurosci Biobehav Rev 2010;34:981–992.
8. Nagasawa T, Juhász C, Rothermel R, et al. Spontaneous and visually driven high-frequency oscillations in the occipital cortex: intracranial recording in epileptic patients. Hum Brain Mapp 2012;33:569–583.
9. Bragin A, Engel J Jr, Wilson CL, et al. Hippocampal and entorhinal cortex high-frequency oscillations (100–500 Hz) in human epileptic brain and in kainic acid-treated rats with chronic seizures. Epilepsia 1999;40:127–137.
10. Staba RJ, Wilson CL, Bragin A, et al. Quantitative analysis of high-frequency oscillations (80–500 Hz) recorded in human epileptic hippocampus and entorhinal cortex. J Neurophysiol 2002;88:1743–1752.
11. Rampp S, Stefan H. Fast activity as a surrogate marker of epileptic network function? Clin Neurophysiol 2006;117:2111–2117.
12. Le Van Quyen M, Khalilov I, Ben-Ari Y. The dark side of high-frequency oscillations in the developing brain. Trends Neurosci 2006;29:419–427.
13. Jirsch JD, Urrestarazu E, LeVan P, et al. High-frequency oscillations during human focal seizures. Brain 2006;129:1593–1608.
14. Ochi A, Otsubo H, Donner EJ, et al. Dynamic changes of ictal high-frequency oscillations in neocortical epilepsy: using multiple band frequency analysis. Epilepsia 2007;48:286–296.
15. Jacobs J, Levan P, Châtillon CE, et al. High frequency oscillations in intracranial EEGs mark epileptogenicity rather than lesion type. Brain 2009;132:1022–1037.
16. Wu JY, Sankar R, Lerner JT, et al. Removing interictal fast ripples on electrocorticography linked with seizure freedom in children. Neurology 2010;75:1686–1694.
17. Akiyama T, McCoy B, Go CY, et al. Focal resection of fast ripples on extraoperative intracranial EEG improves seizure outcome in pediatric epilepsy. Epilepsia 2011;52:1802–1811.
18. Jacobs J, Zijlmans M, Zelmann R, et al. High-frequency electroencephalographic oscillations correlate with outcome of epilepsy surgery. Ann Neurol 2010;67:209–220.
19. Wu JY, Koh S, Sankar R, Mathern GW. Paroxysmal fast activity: an interictal scalp EEG marker of epileptogenesis in children. Epilepsy Res 2008;82:99–106.
20. Kobayashi K, Watanabe Y, Inoue T, et al. Scalp-recorded high-frequency oscillations in childhood sleep-induced electrical status epilepticus. Epilepsia 2010;51:2190–2194.
21. Andrade-Valenca LP, Dubeau F, Mari F, et al. Interictal scalp fast oscillations as a marker of the seizure onset zone. Neurology 2011;77:524–531.
22. von Ellenrieder N, Andrade-Valença LP, Dubeau F, Gotman J. Automatic detection of fast oscillations (40–200 Hz) in scalp EEG recordings. Clin Neurophysiol 2012;123:670–680.
23. Stamoulis C, Gruber LJ, Schomer DL, Chang BS. High-frequency neuronal network modulations encoded in scalp EEG precede the onset of focal seizures. Epilepsy Behav 2012;23:471–480.
24. Melani F, Zelmann R, Dubeau F, Gotman J. Occurrence of scalp-fast oscillations among patients with different spiking rate and their role as epileptogenicity marker. Epilepsy Res 2013;106:345–356.
25. Kobayashi K, Miya K, Akiyama T, et al. Cortical contribution to scalp EEG gamma rhythms associated with epileptic spasms. Brain Dev 2013;35:762–770.
26. Kobayashi K, Jacobs J, Gotman J. Detection of changes of high-frequency activity by statistical time-frequency analysis in epileptic spikes. Clin Neurophysiol 2009;120:1070–1077.
27. Hrachovy RA, Frost JD Jr, Kellaway P. Hypsarrhythmia: variations on the theme. Epilepsia 1984;25:317–325.
28. Jambaqué I, Chiron C, Dumas C, et al. Mental and behavioural outcome of infantile epilepsy treated by vigabatrin in tuberous sclerosis patients. Epilepsy Res 2000;38:151–160.
29. Pellock JM, Hrachovy R, Shinnar S, et al. Infantile spasms: a U.S. consensus report. Epilepsia 2010;51:2175–2189.
30. von Ellenrieder N, Beltrachini L, Perucca P, Gotman J. Size of cortical generators of epileptic interictal events and visibility on scalp EEG. Neuroimage 2014;94:47–54.

31. Zelmann R, Lina JM, Schulze-Bonhage A, et al. Scalp EEG is not a blur: it can see high frequency oscillations although their generators are small. Brain Topogr 2014;27:683–704.

32. Korzeniewska A, Franaszczuk PJ, Crainiceanu CM, et al. Dynamics of large-scale cortical interactions at high gamma frequencies during word production: event related causality (ERC) analysis of human electrocorticography (ECoG). Neuroimage 2011;56:2218–2237.

33. Lachaux JP, Axmacher N, Mormann F, et al. High-frequency neural activity and human cognition: past, present and possible future of intracranial EEG research. Prog Neurobiol 2012;98:279–301.

34. Oka M, Kobayashi K, Akiyama T, et al. A study of spike-density on EEG in West syndrome. Brain Dev 2004;26: 105–112.

Clinical Investigative Study

Temporal Lobe Epilepsy with Amygdala Enlargement: A Morphologic and Functional Study

Shigetoshi Takaya, MD, PhD,[*] Akio Ikeda, MD, PhD, Takahiro Mitsueda-Ono, MD, PhD,[†] Riki Matsumoto, MD, PhD, Morito Inouchi, MD,[‡] Chihiro Namiki, MD, PhD, Naoya Oishi, MD, PhD, Nobuhiro Mikuni, MD, PhD,[§] Koichi Ishizu, MD, PhD, Ryosuke Takahashi, MD, PhD, Hidenao Fukuyama, MD, PhD

From the Radioisotope Research Center, Kyoto University, Kyoto, Japan (ST); Human Brain Research Center, Kyoto University Graduate School of Medicine, Kyoto, Japan (ST, NO, HF); Department of Neurology, Kyoto University Graduate School of Medicine, Kyoto, Japan (AI, TM-O, RM, MI, RT); Department of Psychiatry, Kyoto University Graduate School of Medicine, Kyoto, Japan (CN); Department of Neurosurgery, Kyoto University Graduate School of Medicine, Kyoto, Japan (NM); and Innovation Unit for Near Future System and Technology, Kyoto University Graduate School of Medicine, Kyoto, Japan (KI).

ABSTRACT

BACKGROUND AND PURPOSE

Temporal lobe epilepsy (TLE) with nontumoral amygdala enlargement (AE) has been reported to be a possible subtype of TLE without hippocampal sclerosis (HS). The purpose of this study was to clarify morphologic and functional characteristics of TLE with AE (TLE + AE).

METHODS

We evaluated gray matter volume and cerebral glucose hypometabolism using magnetic resonance imaging (MRI) voxel-based morphometry (VBM) and voxel-based statistical analysis of [^{18}F]-fluorodeoxyglucose positron emission tomography (FDG-PET) images in 9 patients with TLE + AE as compared with controls. For VBM analysis, we recruited 30 age- and sex-matched healthy volunteers as controls. For the comparison of FDG-PET analysis, 9 patients with definite mesial TLE with HS (MTLE + HS), and 16 age- and sex-matched healthy controls were recruited.

RESULTS

In patients with TLE + AE, a significant increase in gray matter volume was found only in the affected amygdala, and no significant decrease in gray matter volume was detected. In addition, significant glucose hypometabolism was observed in the affected amygdala, whereas significant glucose hypometabolism in the hippocampus, a prominent feature of definite MTLE+HS, was not observed.

CONCLUSIONS

TLE + AE is different from MTLE + HS from morphologic and functional points of view, and the enlarged amygdala per se is potentially an epileptic focus in patients with partial epilepsy.

Keywords: FDG-PET, VBM, TLE, hypometabolism, localization-related epilepsy.

Acceptance: Received July 4, 2011, and in revised form October 7, 2011. Accepted for publication November 20, 2011.

Correspondence: Address correspondence to Dr. Shigetoshi Takaya, Radioisotope Research Center, Kyoto University, Yoshidakonoe-cho, Sakyo-ku, Kyoto 606-8501, Japan. E-mail: shig.t@kuhp.kyoto-u.ac.jp.

[*]Currently at Athinoula A. Martinos Center for Biomedical Imaging, Massachusetts General Hospital, Harvard Medical School. [†]Currently at Otsu Red Cross Hospital, Shiga, Japan. [‡]Currently at Kitano Hospital, Osaka, Japan. [§]Currently at Department of Neurosurgery, Sapporo Medical University School of Medicine, Hokkaido, Japan.

Disclosure: None of the authors has any conflict of interest to disclose.

J Neuroimaging 2014;24:54-62.
DOI: 10.1111/j.1552-6569.2011.00694.x

Introduction

Temporal lobe epilepsy (TLE) is the most common localization-related epilepsy in adults. Hippocampal sclerosis (HS) is a well-defined structural abnormality associated with TLE in neuropathologic and neuroimaging examinations. However, a substantial number of patients with clinically diagnosed TLE have no evidence of HS or other structural lesions on conventional magnetic resonance imaging (MRI).[1,2]

Even if no volume or signal intensity abnormalities have been visually detected with conventional MRI, neuropathologic abnormalities in the amygdala with no other pathologic change have been described in temporal lobe specimens resected from patients with intractable TLE.[3,4] Moreover, in vivo quantitative measurement of the amygdala using MRI T2 relaxometry have revealed that a nonnegligible number of patients with "MRI-negative" TLE showed increased T2 signal in the amygdala ipsilateral to the epileptic focus detected by electroencephalography (EEG).[5]

More recently, using high-resolution MRI, TLE with nontumoral amygdala enlargement (AE) has been reported to be clinically different from mesial TLE with HS (MTLE + HS).[6,7] In our previous report, a manual volumetric study of the

amygdala has demonstrated that the AE was a unique condition that was not observed in patients with MTLE + HS and those with extratemporal partial epilepsy (non-TLE), and visual inspection of [^{18}F]-fluorodeoxyglucose positron emission tomography (FDG-PET) images has shown that glucose hypometabolism was observed in the temporal lobe ipsilateral to the AE.[7] However, 2 questions arise concerning patients with TLE with AE (TLE + AE): (1) whether structural abnormality exists outside the amygdala; and (2) whether regional glucose hypometabolism in the interictal period, an indicator of focal cortical dysfunction including epileptogenicity, shows a different topographic pattern from that of MTLE + HS.

MRI voxel-based morphometry (VBM) and FDG-PET can delineate structural and functional abnormalities in the whole brain in vivo. In particular, FDG-PET has demonstrated high sensitivity in detecting epileptic foci in patients with MRI-negative TLE as well as those with MTLE + HS.[1] In this study, we aimed to clarify morphologic characteristics of TLE + AE in the whole brain using VBM, and to explore the difference in the topographic pattern of glucose hypometabolism between TLE + AE and MTLE + HS using voxel-wise statistical analysis of FDG-PET images.

Subjects and Methods

Subjects

We recruited 9 MTLE patients with nontumoral AE and no HS for conventional 1.5 T MRI (TLE + AE group, 7 males; mean age ± standard deviation, 49.3 ± 13.6 years). Patients aged from 20 to 65 years were included. Clinical feature of these patients (patients 1-7) and the result of a manual volumetric study of the amygdala have been reported previously.[7] The diagnosis of TLE was based on the presence of complex partial seizures consistent with TLE,[8] and focal epileptiform discharges predominantly in the temporal area ipsilateral to the AE. Three patients (patients 4, 6, and 9) demonstrated generalized tonic-clonic seizures without aura before carbamazepine was started, but were diagnosed with TLE because consistent epileptiform discharges or EEG seizure patterns arising from the temporal area ipsilateral to the AE were observed in conventional scalp EEG. Patients with the following criteria were excluded: (1) significant past medical history of acute encephalitis/meningitis or severe head trauma; (2) focal neurological abnormalities on physical examination or psychiatric diseases including depression; (3) highly suspected tumoral lesion in MRI where the enlarged amygdala apparently compressed adjacent tissue or showed clear intensity changes in T2-weighted, FLAIR or Gd-enhanced T1-weighted images; (4) morphologic or signal abnormalities outside the amygdala in MRI; and (5) epileptic paroxysms in the extratemporal area on EEG. One patient (patient 7) underwent lesionectomy of the enlarged amygdala, and pathological examination indicated focal cortical dysplasia with mild gliosis.[7] Clinical demographics of patients with TLE + AE in this study are shown in Table 1.

For VBM analysis, we recruited 30 age- and sex-matched healthy volunteers as controls. For the comparison of FDG-PET data, we acquired preoperative FDG-PET data from 9 patients with MTLE + HS who underwent subtemporal amygdalohippocampectomy and became seizure-free after surgery.[9] In all patients, HS was confirmed by pathological examination. Because age groups substantially differed between patients with TLE + AE and those with MTLE + HS, we first recruited 22 healthy volunteers and then selected those 16 subjects as controls who were age- and sex-matched with subjects in each patient group. Ten healthy subjects were overlapping in the both control groups. Patient and control group profiles are summarized in Table 2.

Table 1. Clinical Demographics of Patients with TLE + AE

No.	Age/Sex	Affected Side	Onset	FC	Seizure Type	AEDs(mg)
1	63/M	R	46	–	CPS	CBZ(250)
2	24/F	L	19	–	CPS	CBZ (200), PB (90)
3	57/M	L	49	–	CPS	CBZ (200), VPA (600)
4	32/F	L	32	+	GTC	CBZ (350), VPA (800)
5	63/M	R	61	–	CPS	CBZ (400)
6	45/M	R	44	–	GTC	CBZ (200), VPA (800)
7	53/M	L	51	–	CPS	CBZ (200), DZP (4)
8	53/M	L	52	–	CPS	CBZ (300)
9	57/M	L	55	–	GTC	CBZ (200)

TLE +AE = temporal lobe epilepsy with amygdala enlargement; R = right; L = left; FC = febrile convulsion; AEDs = antiepileptic drugs; CBZ = carbamazepine; PB = phenobarbital; VPA = valproate; DZP = diazepam; CPS = complex partial seizure; GTC = generalized tonic-clonic seizure.
Clinical feature of patients 1–7 and the result of a manual volumetric study of the amygdala have been reported previously [Mitsueda-Ono et al, *J Neurol Neurosurg Psychiatry*. 2011;82(6):652-657].

For the statistical analyses of clinical features, age and sex ratios were compared across groups using an independent sample *t*-test and a Fisher's exact test, respectively.

This study was approved by the Ethics Committee of the Kyoto University Graduate School of Medicine (E 479), and written informed consent was obtained from all subjects.

Imaging Data Acquisition

MRI

For VBM analysis, the 3-dimensional T1-weighted structural images were obtained using a 3 T MRI scanner (Trio, Siemens, Erlangen, Germany) with the following sequence: magnetization-prepared rapid-acquisition gradient-echo sequence, repetition time (TR)/echo time (TE) = 2,000/4.38 ms; inversion time (TI) = 990 ms; flip angle, 8°; matrix size, 240 × 256; field of view, 225 mm × 240 mm; slice thickness, 1.0 mm; number of slices, 208.

PET

FDG-PET scans were performed using a PET scanner (Advance, General Electric Medical Systems, Milwaukee, WI, USA). After fasting for at least 4 hours, patients were intravenously injected with [^{18}F]-FDG at 370 MBq (10 mCi). Then, 40 minutes after the administration of the radiotracer, 35 slices of brain-emission images were acquired over a 20-minute period. The subjects were studied in an awake, resting state, with their eyes closed and their ears unplugged in a dimly lit environment. No abnormal behaviors were observed, and patients did not report any subjective manifestations of

Table 2. The Profiles of Each Group

	TLE + AE	Controls for TLE + AE		MTLE + HS	Controls for MTLE + HS
		MRI	FDG-PET		FDG-PET
Number	9	30	16	9	16
Age ± SD (year)	49.7 ± 13.6	46.8 ± 12.0	45.4 ± 13.3	29.2 ± 11.0	32.0 ± 11.8
Males:Females	7:2	22:8	11:5	4:5	9:7
Affected side (L:R)	6:3	–	–	5:4	–

TLE + AE = temporal lobe epilepsy with amygdala enlargement; MTLE + HS = mesial temporal lobe epilepsy with hippocampal sclerosis; SD = standard deviation.

seizures during the examination. Emission images were reconstructed into a 128 × 128 matrix image with a pixel size of 1.95 × 1.95 mm and a slice thickness of 4.25 mm. All reconstructed images were corrected for attenuation using ^{68}Ge-^{68}Ga transmission scans performed before the actual scan.

Imaging Data Analyses

MRI and FDG-PET images from patients with right TLE + AE and MTLE + HS were flipped horizontally so that the epileptogenic zone was lateralized to the left side. To account for hemispheric asymmetry, the images were flipped in the same proportion of healthy subjects as in each patient group. In statistical analyses, adjustment for the potential confounders of age and sex was performed by including them as nuisance variables in the statistical model, except for the analysis exploring intra-individual hemispheric asymmetry in the FDG-PET study (see later). Patients with TLE + AE have a propensity for mild epileptic history.[7] In patients with mild TLE, morphologic and functional abnormalities are expected to be less severe than in patients with intractable TLE.[10,11] Therefore, to detect subtle changes in patients with TLE + AE, we adopted a relatively less stringent statistical threshold as a default, at voxel level of $P < .005$ and cluster-level corrected for multiple comparisons across the whole brain at $P < .05$.

VBM

We applied VBM standard routines and default parameters implemented in SPM5 (Wellcome Department of Cognitive Neurology, London, UK). This method adopts a unified segmentation algorithm, which comprises spatial normalization, tissue classification, and bias correction within the same generative model.[12] Spatially normalized segmentations were modulated with the Jacobian determinants from the transformation to preserve the total amount of gray matter signal.[13] The results of segmentation were inspected visually in all subjects and no apparent misclassification of tissues was observed in the mesial temporal area. Spatially normalized, modulated gray matter images were then smoothed with an 8-mm full width at half maximum (FWHM) isotropic Gaussian kernel. In statistical analysis, only voxels exceeding the absolute value of .05 were included, and gray matter differences between patients with TLE + AE and controls were assessed using an independent samples t-test.

FDG-PET

The voxel-wise comparison of FDG-PET images was performed using SPM5. Using affine and nonlinear warping, each individual FDG-PET image was spatially normalized to fit the customized FDG-PET template, which is coregistered to the Montreal Neurological Institute (MNI) space. The spatially normalized images were then smoothed with a 12-mm FWHM Gaussian kernel. To remove the effects of global activity, each voxel count was normalized to the total count of the whole brain using proportional scaling. A t-statistic was calculated for the group comparison.

We explored brain regions showing glucose hypometabolism in patients with TLE + AE or MTLE + HS in 3 ways. (1) In comparing each group with controls, an independent samples t-test was performed at voxel level of $P < .005$ and cluster-level corrected for multiple comparisons across the whole brain at $P < .05$. (2) In assessing interhemispheric asymmetry within each group, a dependent samples (paired) t-test was performed at a more stringent statistical threshold, at a height threshold of $P < .05$ corrected for multiple comparisons using the false discovery rate (FDR) algorithm, and an extent threshold of 300 voxels. We adopted a more stringent statistical threshold, expecting the higher statistical power in a dependent samples t-test and less interhemispheric variability in each individual than inter-subject variability in healthy subjects. (3) In directly comparing the TLE + AE and MTLE + HS groups, an independent samples t-test was performed. We adopted a less stringent statistical threshold, at a height threshold of $P < .005$, uncorrected for multiple comparisons, and an extent threshold of 100 voxels, to detect subtle changes in a relatively small number of compared subjects.

The results are displayed on an individual MRI of a healthy subject that is spatially normalized to the MNI space. To preclude the effect of arbitrariness in the choice of statistical threshold uncorrected for multiple comparisons and to clarify differences in the distribution of temporal lobe hypometabolism in each group, an unthresholded T-map of the analysis is also displayed.

Results

Gray Matter Volume

In the TLE + AE group compared to controls, a significant increase in gray matter volume was found in the dorsomedial part of the amygdala ipsilateral to the affected side (Table 3, Fig 1). However, no significant increase or decrease in gray matter volume was detected in any other brain regions including the hippocampus.

Table 3. Brain Region Showing an Increase in Gray Matter Volume in Patients with TLE + AE Compared to Healthy Controls

Anatomical Region	Side	Cluster Size (Voxels)	T Value of the Peak	Peak Coordinate*		
				x	*y*	*z*
Amygdala	I	477	4.97	−12	−11	−20
	I			−14	−10	−11

*Talairach coordinate.
TLE + AE = temporal lobe epilepsy with amygdala enlargement; I = ipsilateral side of the affected temporal lobe.

Glucose Hypometabolism

Compared to controls ($n = 16$), the TLE + AE group ($n = 9$) demonstrated glucose hypometabolism in the amygdala, temporal pole, and the anterior part of the basal temporal area ipsilateral to the affected side, and the dorsomedial part of the bilateral thalami, more so on the ipsilateral side to the affected amygdala. In contrast, the MTLE + HS group ($n = 9$) showed glucose hypometabolism broadly in the anterior part of the affected temporal lobe including the mesial, basal, and lateral temporal area, most prominently in the hippocampus (Table 4, Fig 2). In the assessment of interhemispheric glucose hypometabolism asymmetry within each group, the TLE + AE group demonstrated glucose hypometabolism only in the amygdala ipsilateral to the affected side; the MTLE + HS group showed glucose hypometabolism broadly in the anterior part of the temporal lobe, most prominently in the hippocampus (Table 4, Fig 2). In contrast, no significant intrahemispheric glucose hypometabolism was observed in the both control groups in which the images were flipped in the same proportion of healthy subjects as in each patient group. Unthresholded T-maps indicated the relative preservation of hippocampal glucose metabolism in the TLE + AE group in comparison to the TLE with HS group (Fig 3).

A direct comparison between TLE + AE and MTLE + HS groups revealed decreased glucose metabolism in the MTLE + HS group in the hippocampus ipsilateral to the affected side (Fig 4). The reverse comparison identified no glucose hypometabolism in any regions in the TLE + AE group compared to the MTLE + HS group.

Discussion

The present neuroimaging study demonstrates that patients with TLE + AE have isolated enlargement in the dorsomedial part of the amygdala with no significant volume change in the hippocampus. This morphologic pattern is distinct from MTLE + HS, in which hippocampal atrophy is the most prominent finding.[14,15] It further strengthens the previous finding that TLE + AE could be a subtype of TLE.[6,7] In addition, glucose hypometabolism in patients with TLE + AE was relatively restricted to the affected amygdala, adjacent regions in the temporal lobe, and the bilateral thalami, with greater hypometabolism ipsilateral to the AE. In contrast, significant glucose hypometabolism in the hippocampus, which is a defining feature of MTLE + HS,[16,17] was not observed in TLE + AE patients.

Volume Change

Many studies have investigated morphologic changes in patients with MTLE + HS. Consistent findings include gray matter atrophy in the mesial temporal lobe, including the amygdala as well as the hippocampus ipsilateral to the affected side and other remote brain regions involved in seizure propagation.[14,15,18,19] Mesial temporal atrophy is a common finding even in mild drug-responsive MTLE + HS and MRI-negative TLE.[19-21] In the patients included in this study, morphologic abnormality was limited to the amygdala. According to neuropathological and neuroimaging studies, abnormalities in the amygdala can coexist with HS in patients with MTLE + HS.[5,7,18,22] However, the presence of histopathological HS can be highly predicted by volumetric MRI.[2,23] Thus, concomitant HS is rather unlikely in the patients with TLE + AE included in this study.

In some studies, an increase in gray matter volume outside the mesial temporal regions has been observed in patients with MTLE + HS or MRI-negative TLE, which has been assumed to result from diminished gray-white matter demarcation.[14,19] The process of tissue classification in VBM is subject to error at the interface between tissue types, where the border of gray and white matter is blurred.[24] However, in the present study, we found an increase in gray matter volume in the dorsomedial part of the amygdala, which borders CSF. Moreover, we observed no apparent misclassification of tissues in this area by visual

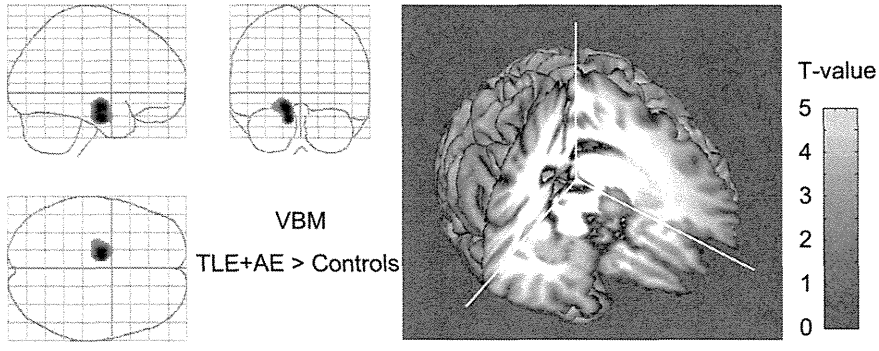

Fig 1. A brain region showing increased gray matter volume in patients with TLE with AE compared to age- and sex-matched healthy controls. Results are thresholded at voxel level of $P < .005$ and cluster-level corrected for multiple comparisons across the whole brain at $P < .05$. A significant region is displayed on a glass brain template (left-hand side) and a spatially normalized individual brain (right-hand side).

Table 4. Brain Regions Showing a Decrease in Glucose Metabolism

	Cluster Size (Voxels)	T value of the Peak	Peak Coordinate**			Side	Anatomical Region
			x	y	z		
Comparison with controls*							
TLE + AE controls	1,341	6.12	−6	−21	12	I	Thalamus (dorsomedial part)
		5.07	12	−9	13	C	Thalamus (dorsomedial part)
	1,750	5.29	−59	5	−25	I	Temporal pole
		4.31	−28	6	−42	I	Basal temporal area
		4.00	−24	0	−34	I	Amygdala
MTLE + HS controls	6,383	7.19	−30	4	−41	I	Basal temporal area
		7.05	−32	14	−36	I	Temporal pole
		7.03	−34	−18	−18	I	Hippocampus
	1,117	4.59	−2	45	3	I	Medial frontal gyrus
		3.63	−2	68	−8	I	Frontal pole
		3.39	0	23	23	I	Anterior cingulate gyrus
Hemispheric asymmetry							
TLE + AE	596	9.82	−26	−3	−23	I	Amygdala
		6.44	−32	7	−15	I	Amygdala
MTLE + HS	8,045	17.82	−30	−16	−14	I	Hippocampus
		12.23	−32	−2	−30	I	Uncus
		12.19	−6	34	−19	I	Medial frontal gyrus
Direct comparison							
MTLE + HS TLE + AE	154	3.61	−28	−13	−20	I	Hippocampus

*Controls were age- and sex-matched healthy volunteers for each patient group.
**Talairach coordinate.
TLE + AE = temporal lobe epilepsy with amygdala enlargement; MTLE + HS = mesial temporal lobe epilepsy with hippocampal sclerosis; I = ipsilateral side of the affected temporal lobe; C = contralateral side of the affected temporal lobe.

inspection. Thus, this finding is less likely to be attributable to misclassification in the segmentation process.

Glucose Hypometabolism in the Amygdala and Thalami

The amygdala is susceptible to kindled seizures in animals,[25] and direct stimulation of the amygdala causes complex partial seizures in humans as observed well in hippocampus.[26] The initiation of seizure in the amygdala has been observed in intraoperative depth electrode studies. Epileptic activity then propagates rapidly from the amygdala to the hippocampus, and patients demonstrate ictal manifestations similar to those of hippocampal origin.[27,28] In addition, consistent differences have been little identified in ictal manifestations or auras between patients with pathologically defined amygdala sclerosis (HS-negative) and those with HS.[3] Thus, differentiation of the seizure-onset zone between seizures of hippocampal and amygdalar origin may be impossible from the viewpoint of seizure semiology.

FDG-PET has demonstrated high sensitivity in detecting the epileptic focus even in patients with MRI-negative TLE.[1] In this study, glucose hypometabolism was detected in the amygdala and adjacent regions in the affected temporal lobe and in the bilateral thalami, more so on the affected side. Glucose hypometabolism in the thalamus has been reported in localization-related epilepsies and assumed to be a secondary hypofunction. From these lines of evidence, the amygdala is likely to be a primary epileptic focus of TLE in our patient cohort.[7]

The observation of glucose hypometabolism in the bilateral thalami, particularly ipsilateral to the AE, is another point of interest in this study. Electrophysiological studies have demonstrated the thalamic involvement during TLE seizures, especially arising from the mesial temporal structures.[29] Glucose hypometabolism in the thalamus ipsilateral to the affected side is known to be associated with a long seizure duration.[30] However, in most patients in this study, the clinical onset of epilepsy was middle age, and FDG-PET scanning was performed within a few years after onset. This may imply that the epileptogenicity in the amygdala was mild and developed slowly, thus the subclinical epileptic activity had been present for decades before onset. This assumption is consistent with the fact that seizures have been well controlled with a low dose of antiepileptic drugs in the patients with TLE + AE included in this study.[7] The assumption of long-lasting mild epileptic activity in the amygdala may be a clue to speculate the possible etiology of the TLE + AE as discussed later. On the other hand, bilateral involvement of the thalamus has been assumed in idiopathic generalized epilepsy by means of EEG-fMRI study in humans.[31] In this study, 3 patients with TLE + AE experienced generalized tonic-clonic seizures without aura. The dorsomedial nucleus of the thalamus has dense reciprocal connections with the amygdala,[32] and has been thought to function as a node of limbic seizure propagation from an epileptic focus in the mesial temporal lobe.[33] Glucose hypometabolism in the dorsomedial part of the bilateral thalami in patients with TLE + AE might indicate that the epileptic activity emanating from the amygdala has a propensity to propagate rapidly to the thalamus, which triggers thalamo-cortical interplay and causes generalized seizures. However, since there is no report showing glucose hypometabolism in the thalami in patients with idiopathic generalized epilepsy,[34] the discussion remains to be further investigated.